THE ASTROPHYSICAL JOURNAL, 328:523–529, 1988 May 15

BROAD-LINE VARIABILITY IN NGC 5548

T. KALLMAN AND M. ELITZUR[1]
Laboratory for High Energy Astrophysics, NASA/Goddard Space Flight Center
Received 1987 June 8; accepted 1987 November 3

ABSTRACT

Wd discuss the possible explanations for the variability behavior of the He II λ4686 and Hβ lines in the Seyfert galaxy NGC 5548 as observed by Peterson and Ferland. We explore the range of variability expected from these lines according to the standard models for broad-line clouds, assuming changes in the values of various of the clouds' defining parameters. When compared with model predictions the observed line variability suggests the existence of a strong, variable EUV component of the ionizing spectrum and of two populations of clouds which differ in their velocity distributions and in their response to continuum variations.

Subject headings: galaxies: individual (NGC 5548) — galaxies: Seyfert

I. INTRODUCTION

The Seyfert galaxy NGC 5548 is noted for its broad-line variability (Ulrich and Boisson 1983; Barr, Willis, and Wilson 1981). One example of this behavior is the flaring event in the optical continuum closely followed by an increase in the flux of He II λ4686 line observed by Peterson and Ferland (1986). A possible explanation for this event, advocated by Peterson and Ferland (1986), is that it was due to a change in the distribution of broad-line gas; that is, that gas suddenly appeared in the broad-line region under conditions which caused it to radiate preferentially in the He II λ4686 line, and that this same gas may have been responsible for the continuum flare as it was accreted onto the central compact object.

Other origins for line variability may also be at work in NGC 5548. Although the line spectrum emitted by a single cloud can respond essentially instantaneously to changes in the ionizing continuum, the response of the observed spectrum (which gets contributions from many clouds) to continuum changes will be smeared and delayed by light travel time effects. The observed line spectrum at any given time can depend on the history of the continuum flux and shape. Furthermore, if there exists a distribution of cloud pressures and incident fluxes then the emitted line spectrum may vary from one cloud to another. The observed line spectrum will then depend sensitively on which clouds dominate the total spectrum.

The perils associated with interpreting apparent correlations between lines and continua have been emphasized by Krolik (1987). In particular, any attempt at an exhaustive discussion of correlated variability requires analysis of spectra taken at time intervals whose spacing is small compared to the shortest variability time scale observed and which span a period which is much greater than the longest time scale of interest. Since the published data on NGC 5548 do not permit such an analysis, in this paper we will discuss the salient features of the Ferland and Peterson data, compare them with simple models for the broad-line region and discuss the consequences that the various origins of variability would have for our understanding of the broad emission-line regions (BLR) of quasars and other active galactic nuclei. Our conclusions which depend on the existence of correlated line and continuum variability must therefore be considered tentative pending an accurate measurement of the line-continuum covariance function for NGC 5548. Further impetus for studies such as this is provided by observations of variability in emission lines from other active galaxies (e.g., Alloin, Boisson, and Pelat 1987).

II. CLOUD PHYSICS

Necessary to any discussion of line variability is an understanding of the physics of emission properties of broad-line clouds. The properties of these clouds, which have been thoroughly reviewed by many authors (e.g., Davidson and Netzer 1978; Ferland and Shields 1985; Kwan and Krolik 1982; Kwan 1984; Mushotzky and Ferland 1984, and references therein), and which we will take as given, include the following: clouds exist in a spherical distribution around an isotropically-emitting source of ionizing continuum radiation. The covering fraction, defined as the fraction of the solid angle subtended by the clouds as seen from the source is $C \approx 0.1$. Model clouds are parameterized by their gas pressure P, ionization parameter Ξ (defined as the ratio of the incident flux in the ionizing continuum to the gas pressure and the speed of light; see, e.g., Krolik, McKee, and Tarter 1981), column density N, and incident spectral shape. We use the same element abundances as Kwan and Krolik (1981). Models with $P = P_{\rm std} \approx 0.03$ dyne cm^{-2}, $\Xi = \Xi_{\rm std} \approx 0.3$, and $N = N_{\rm std} \approx 10^{23}$ cm^{-2} heated and ionized by a "double power law" ionizing spectrum $L_E = Lf_E$ (ergs s^{-1} ergs^{-1}), with $\int dEf_E = 1$, and

$$f_E \approx \begin{cases} E^{-1.2}, & E < 2 \text{ keV}; \\ E^{-0.7}, & E > 2 \text{ keV}; \end{cases} \quad (1)$$

are generally successful in reproducing the strengths of the strongest lines in an ensemble of AGN spectra (see, however, Netzer 1985). Model clouds may be divided into two spatial regions: In the H II zone are emitted the lines from multiply charged ions such as He II, O VI, N V, and C IV. The ionization structure, temperature, and emission in this zone depend primarily on ionization parameter. The "extended ionized zone" is the principal emission site for the strong lines of neutral and singly ionized species, such as the hydrogen Balmer lines (although these can also be influenced by recombination emission in the H II zone), Fe II lines, and Mg II λ2798. The line intensities emitted from the extended ionized zone depend most sensitively on the cloud pressure, P, owing to the impor-

[1] Also Department of Physics and Astronomy, University of Kentucky.

tance of collisional excitation and ionization. The ionization front separating the two regions lies at a distance from the illuminated face given by $\sim 10^{12}(\Xi/\Xi_{\rm std})(P_{\rm std}/P)$ cm. This corresponds to a column density of 10^{22} cm^{-2} at the fiducial values of Ξ and P. The relative importance of the radiation from the H II zone and the extended ionized zone depends on the ionization parameter, the gas pressure, and on the shape of the incident spectrum. The dependence on the spectral shape is particularly apparent in the fluxes of the lines formed in the extended ionized zone, since the heating in this zone is produced by (>1 keV) X-ray absorption. For example, incident spectra that lack X-rays will excite Balmer lines only by recombination in the H II zone.

All of the cloud models discussed in this paper are stable against the effects of disruption by radiation pressure from internally generated line photons (Elitzur and Ferland 1986), according to the criterion $P_{\rm rad} < P_{\rm tot}$. It should be pointed out that this is different from the more restrictive criterion $P_{\rm rad} < P_{\rm gas}$ (equivalent to $P_{\rm rad} < 1/2P_{\rm tot}$) employed by Elitzur and Ferland. The reasoning behind their choice was that although equilibrium solutions are possible in the region $P_{\rm gas} < P_{\rm rad} < P_{\rm tot}$, that equilibrium would be unstable. However, this point has not yet been fully explored in a detailed stability analysis which is why we choose the more conservative—and more certain—stability criterion.

The two numbers of primary interest in the case of NGC 5548 are the ratio of the strengths of the He II λ4686 and Hβ lines, and the reprocessing efficiency of one of them, say Hβ. We define this latter quantity as

$$\varepsilon_{\rm H\beta} = \frac{F_{\rm H\beta}}{F_{\rm ion}}, \qquad (2)$$

where $F_{\rm H\beta}$ is the Hβ flux emitted by a cloud, and $F_{\rm ion}$ is the ionizing continuum flux incident on the cloud. For a given choice of ionizing spectrum both the He II λ4686/Hβ ratio and the Hβ reprocessing efficiency vary only weakly with cloud parameters (pressure, ionization parameter, and column density) for values of these parameters near the standard ones. That is, the emitted fluxes in both lines are approximately proportional to the ionizing continuum flux. The clouds may be regarded as linear reprocessors of the incident continuum, and we shall refer to them as such in our subsequent discussions.

For cloud parameters which differ from the standard ones by more than a factor of $\sim$10, say, or for ionizing continua significantly different from the double power law, the line-reprocessing efficiencies may differ significantly from standard values. Under these conditions the lines may no longer be regarded as linear reprocessors of the incident continuum. For example, at ionization parameters $\Xi < \Xi_{\rm std}/10$ helium is primarily neutral at the illuminated face of the cloud. The abundance of He II varies as the product of two photoionization rates, so that the He II λ4686 reprocessing efficiency is proportional to Ξ. At high incident continuum fluxes the reprocessing efficiency of Hβ decreases (the Hβ flux approaches a constant value) owing to the fact that the hydrogen atomic level populations approach their thermal equilibrium values. Ionizing spectra with much greater flux in the EUV than the double power law excite more line emission in the H II zone than in the extended ionized zone. The Balmer line emission efficiencies from clouds illuminated by such spectra are nearly constant, and the He II λ4686/Hβ ratio is roughly proportional to the relative numbers of incident photons in the He II and hydrogen Lyman continua. Clouds with column densities less than $\sim 10^{22}$ cm^{-2} (for standard Ξ and P) will have no ionization front and extended ionized zone. Such clouds will radiate a greater He II λ4686/Hβ ratio than thicker clouds, but the reprocessing efficiency of Hβ will be lower than for thicker clouds.

These principles are illustrated in the results shown in Figures 1 and 2. Figure 1 shows the dependence of the reprocessing efficiencies of several observable lines: He II λ4686

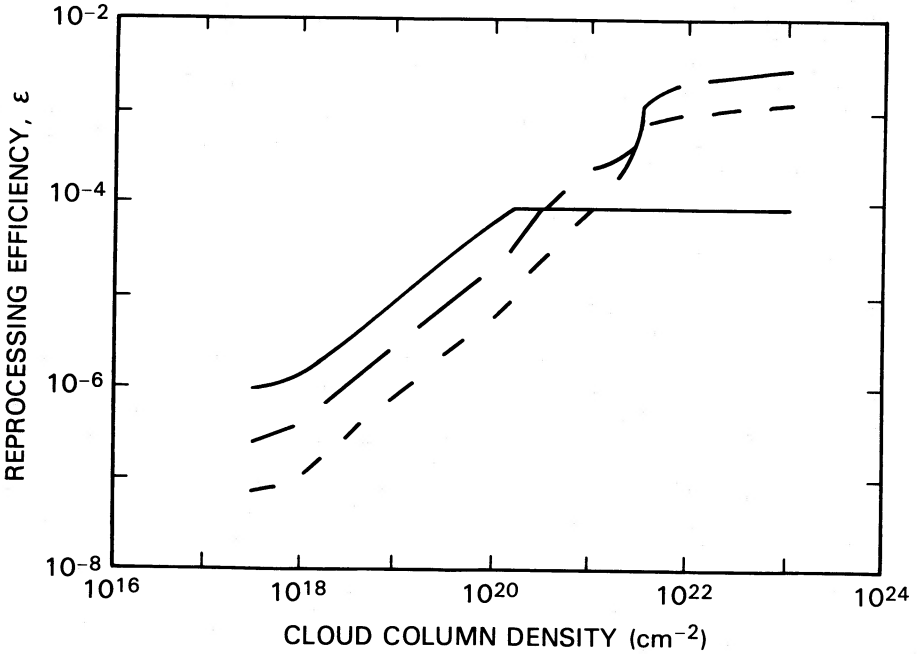

FIG. 1.—Reprocessing efficiency of Hβ, (*long dashed curve*) He II λ4686 (*solid curve*) and He I λ5876 (*short-dashed curve*) lines as a function of cloud column density

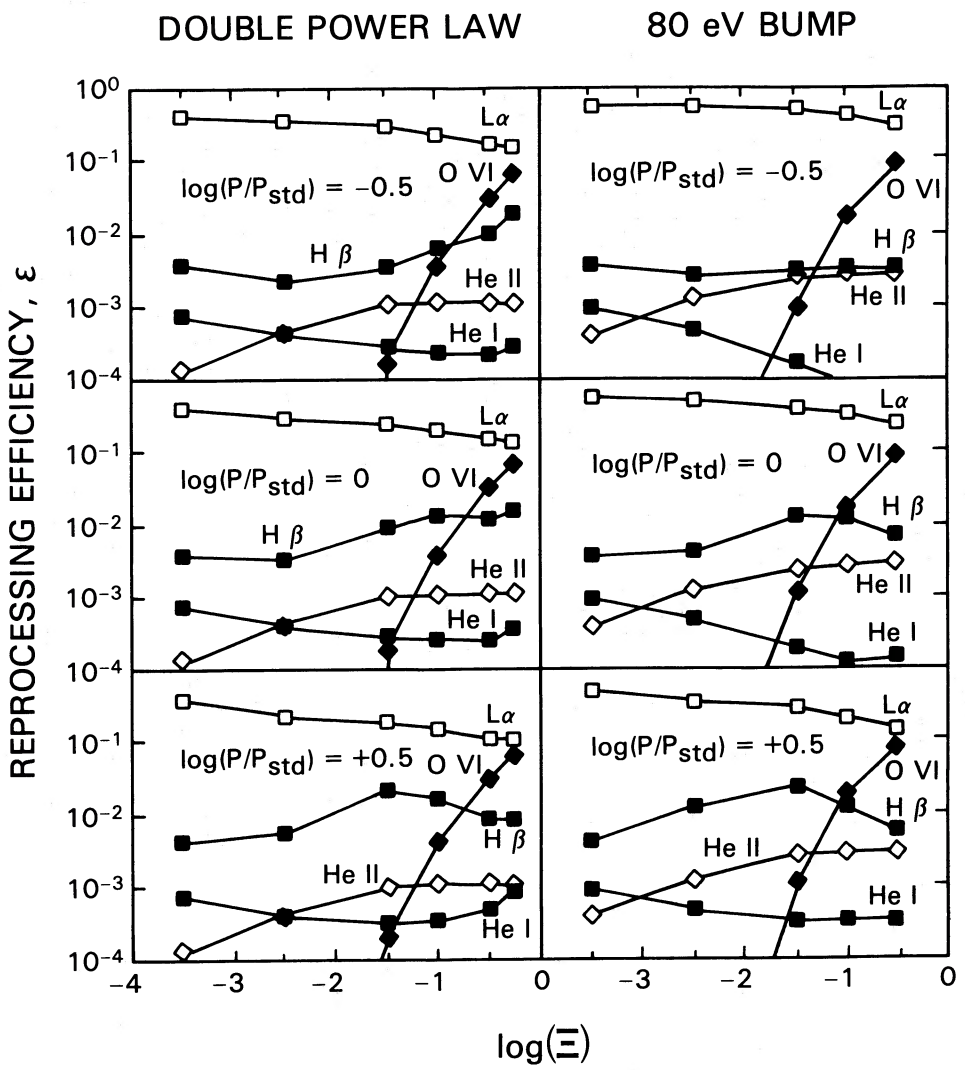

FIG. 2.—Reprocessing efficiency of Lα, Hβ, He II λ4686, He I λ5876, and O VI λ1034 lines as a function of cloud ionization parameter for two choices of incident ionizing spectrum discussed in the text. Panels correspond to increasing pressure from top to bottom: log $(P/P_{std}) = -0.5, 0., 0.5$.

(*solid curve*), Hβ (*long dashed line*), and He I λ5876 (*short dashed line*) on the cloud column density, for cloud ionization parameter Ξ_{std}, pressure P_{std}, and for column densities less than 10^{23} cm^{-2}. Figure 2 displays the dependence of reprocessing efficiencies of He II λ4686, Hβ, He I λ5876, Lyα, and O VI λ1034, on cloud ionization parameter, pressure, and incident spectrum. All the model results shown in Figure 2 are for clouds with total column density of 10^{23} cm^{-2}. Figure 2*a* assumes a nonthermal double power-law ionizing spectrum of the form described above. Figure 2*b* assumes an EUV-dominated ionizing spectrum similar to that expected from an accretion disk (Krolik and Kallman 1988): $f_E \approx E^{1/3} \exp(-E/80\ \text{eV})$ superposed on the nonthermal double power law. The relative normalization is chosen so that the optical-X-ray spectral index is $\alpha_{ox} = 1.4$. In what follows we will refer to this spectrum as the "80 eV bump." The gas densities (H atoms cm^{-3}) at the illuminated faces of these model clouds for log $(\Xi) = -0.5$ are log $(n) = 9.59$ and 9.61 in the 80 eV bump and double power-law cases, respectively. Clearly apparent in these figures are the features already discussed: The He II λ4686 line, formed by recombination in the H II zone, has a nearly constant reprocessing efficiency when the ionization parameter exceeds some critical value, log $(\Xi) > -1.5$. At ionization parameters lower than this value helium is primarily neutral at the illuminated face of the cloud. The abundance of He II varies as the product of two photoionization rates, so that the He II λ4686 reprocessing efficiency is proportional to Ξ. The efficiency is higher in the thermal spectrum case (Fig. 2*b*) than in the nonthermal case (Fig 2*a*) by about a factor of 2 owing to the greater number of EUV continuum photons in the thermal case. The O VI ion abundance, and hence the λ1034 reprocessing efficiency, depends sensitively on ionization parameter. The effects of collisions dominate the behavior of the Hβ and He I λ5876 lines. At low pressure in the 80 eV bump case Hβ is formed by recombination, so its efficiency is nearly constant with ionization parameter. A power-law spectrum produces some collisional excitation of this line in the extended ionized zone. At high pressures collisional deexcitation causes the Hβ and He I

λ5876 emitted fluxes to vary slowly with the incident continuum flux, so the reprocessing efficiencies are constant or slowly decreasing functions of ionization parameter.

III. OVERVIEW OF THE OBSERVATIONS

The important features of the observations of NGC 5548 as described by Peterson and Ferland (1986) are as follows: prior to the continuum flare which occurred during 1984 March the relative strengths of the Hβ and He II λ4686 lines and their equivalent widths were typical for a composite of quasar spectra: He II λ4686/Hβ ≈ 0.03–0.05, and $W(\mathrm{H}\beta) \approx 170$ Å. Following the flare the Hβ flux had increased by ∼20%, the continuum flux in the vicinity of the lines had increased by ∼70%, and the He II λ4686 flux had increased by a factor of ∼10. The He II λ4686 width increased by a factor of ∼1.5. The flux and width of the He I λ5876 did not change significantly during the time of the flare.

Further insight into the nature of the broad-line changes in NGC 5548 can be gained by comparing the observed changes in the Hβ and He II λ4686 lines with the changes expected from the simple, conventional broad-line cloud models. As we have shown these models predict that, if the cloud parameters do not change significantly from the standard ones, the equivalent widths of the two lines should remain constant as the adjacent continuum varies. This idea can be tested by evaluating the linearity of the Hβ and He II λ4686 lines. We have performed this test by the following procedure: denote by $F_0(\lambda)$ and $F_1(\lambda)$ the observed fluxes before and after the flare, respectively, and by F_0 and F_1 the corresponding fluxes at some fiducial wavelength away from the lines. We then construct the *scaled difference*:

$$F(\lambda) = F_0(\lambda) - (\mathsf{F}_0/\mathsf{F}_1)F_1(\lambda) .$$

The continuum has been eliminated from the quantity $F(\lambda)$, as well as that part of the lines which responds linearly to changes in the continuum. We refer to the residual, $F(\lambda)$, as the "nonlinear component" of the line spectrum; it is displayed in Figure 3. If the lines were truly linear reprocessors this quantity would be identically zero. In fact, it is clear that the nonlinear behavior is present in both the Hβ and He II λ4686 lines. Furthermore, the strengths of the lines are roughly comparable in this difference spectrum (He II λ4686/Hβ ≈ 0.8). The widths are similar to each other in this difference spectrum and to the width of the He II λ4686 line following the flare, FWHM ≈ 120 Å. In contrast, the width of the Hβ line following the flare is FWHM ≈ 78 Å.

The differences between the Hβ line width prior to the flare and the widths of the nonlinear components indicate origins in different populations of clouds for the two line components. The apparent broadening of the He II λ4686 line following the flare implies that the emission in this line following the flare is predominantly from nonlinearly reprocessing clouds, while the Hβ line emission is dominated by linearly reprocessing clouds both before and after the flare. Prior to the flare we can set an upper limit on the contribution of non-linearly reprocessing clouds by assuming that the He II λ4686 emission is dominated by these clouds.

This analysis allows us to evaluate quantitatively the relative values of the important quantities characterizing the line spectrum: the fluxes of Hβ and He II λ4686 from the linear and nonlinear cloud components before and after the flare:

$R_1 = 0.01$–0.05 , He II λ4686 prior to the flare/Hβ prior to the flare;
$R_2 = 0.2$–0.3 , He II λ4686 following the flare/Hβ following the flare;
$R_3 = 0.15$–0.2 , nonlinear Hβ following the flare/Hβ prior to the flare;
$R_4 < 0.05$, nonlinear Hβ prior to the flare/Hβ prior to the flare;
$R_5 = 0.8$–1.0 , nonlinear He II λ4686 following the flare/nonlinear Hβ following the flare.

Further information about the reprocessing clouds can be obtained from the equivalent widths of the lines. We define the reprocessing efficiency of a given line, ε, as the ratio of the line flux at the surface of a cloud to the incident ionizing continuum (energy) flux. This quantity may then be expressed in terms of the cloud covering fraction C and the observed line equivalent width W according to

$$\varepsilon_{\mathrm{H}\beta} = \frac{W}{\lambda \kappa C} , \qquad (3)$$

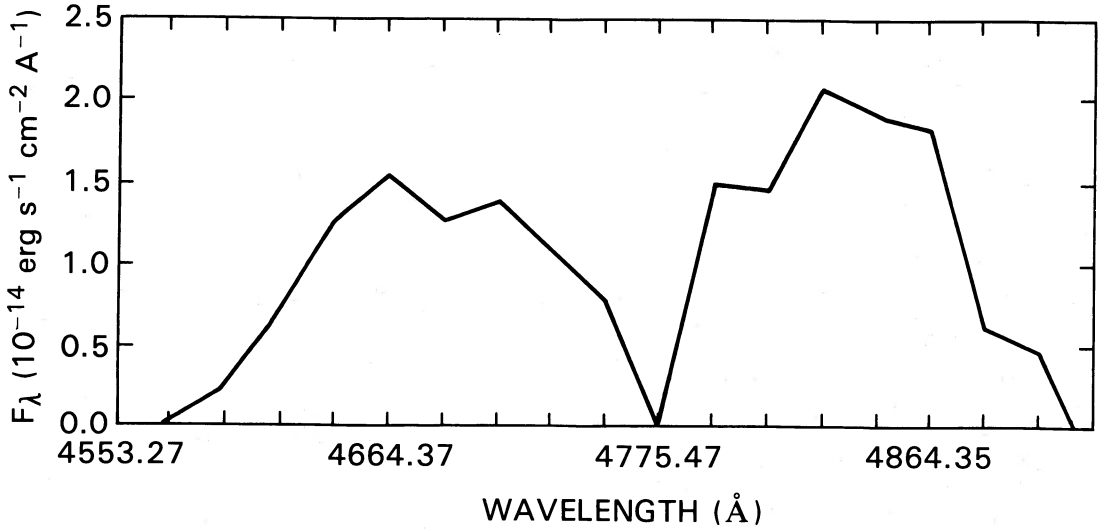

FIG. 3.—The nonlinearly varying part of the NGC 5548 spectrum

where the spectral shape correction factor κ is the ratio of the continuum flux incident on the clouds at 5500 Å to that at 2000 Å. For a double power-law spectrum of the form described in the previous section extending to 5500 Å, κ is 2.9. For a double power-law spectrum of the form described in the previous section for $\lambda < 912$ Å and which is flat for $\lambda > 2000$ Å, $\kappa = 9.8$. The 80 eV bump spectrum has $\kappa = 18.4$ if extended to 5500 Å.

The equivalent width of the Hβ line is $W_{H\beta} \approx 170$ Å prior to the flare; following the flare $W_{H\beta} \approx 110$ Å. The nonlinear part of the Hβ line after the flare has $W_{H\beta} \approx 26$ Å.

IV. THE CLOUDS

The results of the previous section have shown that the variability in the lines of NGC 5548 may be interpreted as coming from two types of clouds: those which respond linearly to changes in the continuum in the vicinity of 5500 Å, and those with a nonlinear response. In this section we discuss, in the context of standard photoionization models, the inferences which the line ratios and equivalent widths allow us to make about the cloud conditions.

As discussed in the previous section, the observed line strengths prior to and following the flare provide us with the reprocessing efficiency of the Hβ line and the He II λ4686/Hβ ratio. Figure 4 displays the regions of the He II λ4686/Hβ which are allowed by the observations prior to the flare (*horizontal hatched region*), after the flare (*vertically hatched region*), and for the nonlinearly varying clouds (*diagonally hatched region*). Also shown are the values of $\varepsilon_{H\beta}$ and He II λ4686/Hβ provided by the various cloud models discussed in § II: clouds with column density 10^{23} cm^{-2} illuminated by the double power-law ionizing spectrum (*open squares*), similar clouds illuminated by the 80 eV bump spectrum (*diamonds*), and clouds with column density less than 10^{23} cm^{-2} illuminated by the double power-law spectrum (*filled squares*). These are a different representation of the model results shown in Figures 1 and 2.

Prior to the flare the He II λ4686/Hβ ratio is 0.02–0.05. The equivalent width implies a reprocessing efficiency $\varepsilon_{H\beta} =$ 0.008–0.012 for $C\kappa = 1$. Figure 4 shows that the measured He II λ4686/Hβ is consistent with cloud models illuminated by the double power law if $\varepsilon_{H\beta} \approx 0.02$. This, together with the measured equivalent width, implies $C\kappa = 0.5$. Such models have pressure slightly greater than the standard value, $P/P_{std} \approx 3$, and ionization parameter slightly less than standard, $\Xi/\Xi_{std} \approx 0.3$. For $\kappa \approx 3$, i.e., for the double power law extending to 5500 Å, this is consistent with $C \approx 0.15$ as suggested by Peterson and Ferland (1986). The observed He II λ4686/Hβ ratio can also be provided by models which have very low ionization parameter, $\Xi/\Xi_{std} \approx 0.01$ at a much lower efficiency, $\varepsilon_{H\beta} \approx 0.003$. These clouds would require $C\kappa \approx 10$, implying either $C \approx 1$ or a value for the shape correction factor κ which is larger than those considered in the previous section. Such values of κ would imply an inverted continuum spectrum in the 5500–2000 Å spectral region. This is not consistent with the observed continuum shape (Barr, Willis, and Wilson 1981).

Following the flare the He II λ4686/Hβ ratio is 0.2–0.3. The equivalent width implies a reprocessing efficiency $\varepsilon_{H\beta} =$ 0.005–0.009 for $C\kappa = 1$. The increased value of He II λ4686/Hβ is consistent with the double power-law models with values of $\varepsilon_{H\beta} \approx 0.003$. Such models have pressures and ionization

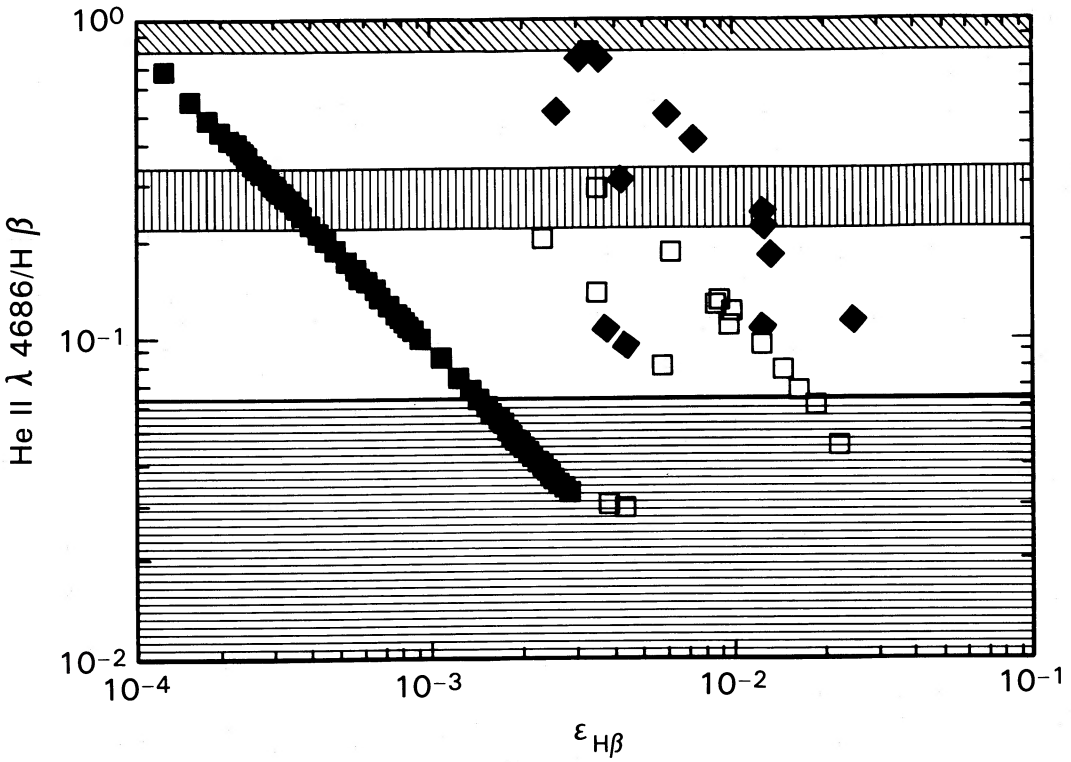

FIG. 4.—The loci of the observed and calculated values of He II λ4686/Hβ and $\varepsilon_{H\beta}$. horizontal hatching corresponds to the observed values before the flare, vertical hatching corresponds to observed values after the flare, and diagonal hatching corresponds to the nonlinearly varying part of the spectrum observed after the flare. Calculated values are for model clouds illuminated by the double power-law spectrum (*open squares*), the 80 eV bump spectrum (*diamonds*), and for low-column density models (*filled squares*).

parameters slightly lower than standard, $P/P_{\rm std} \approx 0.3$. Clouds illuminated by the 80 eV bump spectrum can also account for the increase in He II λ4686/Hβ; such clouds radiate $\varepsilon_{\rm H\beta} \approx 0.011$. The observed equivalent width following the flare and the κ value appropriate to the 80 eV bump spectrum are both consistent with the same covering fraction inferred before the flare, $C \approx 0.1$–0.15.

The nonlinearly emitting clouds have He II λ4686/H$\beta \approx 0.8$–1, which is also consistent with the results of model clouds illuminated by the 80 eV bump if the gas pressure is larger than standard. High pressures serve to collisionally deexcite Hβ and thereby enhance the He II λ4686/Hβ ratio. The efficiency of such models is $\varepsilon_{\rm H\beta} \approx 0.003$. The measured equivalent width then implies $C \approx 0.08$ if κ is the same as for the 80 eV bump.

Figure 4 shows that model clouds with column densities $\sim 10^{21}$ cm^{-2} can provide the large values of He II λ4686/Hβ implied by the observations after the flare, although at low Hβ reprocessing efficiencies. Figure 2 shows that low column density models can provide He II λ4686/H$\beta > 0.1$ if $\varepsilon_{\rm H\beta} < 0.0005$. As pointed out by Peterson and Ferland this low reprocessing efficiency, together with the observed postflare He II λ4686/Hβ ratio, implies $C\kappa \approx 30$. Thus, even if the covering fraction has its maximum possible value, $C \approx 1$, the spectrum in the 2000–912 Å region must increase more steeply than the $E^{1/3}$ slope of the 80 eV bump. In § II it was shown that a further difficulty with low column density clouds is that only a narrow range of column density parameter space provides even such marginally acceptable consistency with the data: if the column density is less than $\sim 10^{21}$ cm^{-2} the reprocessing efficiency is so low as to require $C \gg 1$. If the column density is much greater than 10^{21} cm^{-2} the He II λ4686/Hβ ratio exceeds the observed values.

We can summarize the results of this section as follows: the line strengths before and after the flare, and the nonlinear line components, can be reasonably accommodated by at least one set of model cloud parameters. The line spectrum prior to the flare is consistent with clouds having roughly standard pressure, ionization parameter, and column density illuminated by a double power-law spectrum. Alternatively, these clouds could have a much lower-than-standard ionization parameter, and a much lower line reprocessing efficiency. The line strengths following the flare are consistent with that expected from clouds illuminated by the double power-law spectrum at lower-than-standard values of cloud pressure and ionization parameter or at low column density. Such models all have low reprocessing efficiency. Alternatively, an EUV–dominated ionizing spectrum can provide the observed ratios at higher efficiency. The large He II λ4686/Hβ ratio radiated by the nonlinear clouds can be produced by either EUV-illuminated clouds at moderate efficiency, or by very low column density clouds at very low reprocessing efficiency.

V. ORIGINS OF VARIABILITY: LINE STRENGTHS

We can now discuss various possible scenarios for what happened to the broad-line clouds during the flare of 1984 March. From the discussion so far it is clear that the line spectrum changes imply a change in at least one of the parameters describing the clouds. We discuss them in the following order: (1) scenarios in which the clouds' ionization parameter changed; (2) scenarios in which the clouds' column density and covering fraction changed; and (3) scenarios in which the illuminating spectrum changed. We also distinguish between cloud parameters which are *intrinsic*, i.e., pressure, column density, covering fraction, and distance from the continuum source, and those which are *extrinsic*, i.e., the shape and flux of the ionizing continuum. Each scenario implies changes in the strengths of other emission lines, primarily UV resonance lines, which allow them to be tested by future simultaneous UV and optical spectroscopy of flaring events.

In the first scenario the line changes resulted from a change in the clouds' ionization parameter. If so, the clouds prior to the flare must have had $C \approx 1$, $P \approx P_{\rm std}$, $\Xi \approx \Xi_{\rm std}/10$ illuminated by the double power law. The spectrum after the flare could be accounted for by a factor of ~ 10 increase in the ionization parameter, for the same choice of covering fraction, pressure, and illuminating spectrum. Note that this could be accomplished by either a change in an intrinsic parameter of the clouds, i.e., by a decrease in the clouds' pressure by a factor ~ 10 or a decrease in the clouds' distance from the continuum source by a factor $\sim\sqrt{10}$, or by a change in an extrinsic parameter, i.e., by an increase in the ionizing continuum flux by a factor ~ 10. The extrinsic change implies a change in the spectral shape correction factor, κ, since the continuum flux in the vicinity of 5500 Å was observed to vary by only a factor of 0.7. This scenario is appealing in that it does not require the presence of a strong unseen EUV component to the ionizing spectrum. However, it does require a large covering fraction, owing to the low He II λ4686 reprocessing efficiency at low ionization parameters. At low ionization parameters many UV resonance lines, such as C IV λ1549, are much weaker than at standard ionization parameters. If this scenario is correct future simultaneous UV and optical spectra during flaring events of this type would reveal greater variability in the UV resonance lines than in He II λ4686, with strengths prior to the flare far less than standard (relative to Lyα). Following the flare the UV resonance line strengths are predicted to be roughly standard.

In the second scenario the large He II λ4686/Hβ ratio following the flare is due to clouds with low column density. These clouds radiate with such low efficiency that they must have covering fraction $C \approx 1$; the appearance of these clouds must accompany the flare. This is the scenario suggested by Peterson and Ferland (1986). It requires a change in only the intrinsic parameters of the clouds, and it suffers from the requirement that two cloud parameters, covering fraction and column density, change simultaneously. Unit covering fraction also conflicts with the apparent lack of continuum absorption in NGC 5548 (Reichert *et al.* 1985). It also implies that other lines which are emitted by low column density clouds, such as the UV resonance lines O VI λ1034, N V λ1240, and C IV λ1549, would flare along with He II λ4686. This behavior is predicted to differ from that of the first scenario in that these lines would have standard strengths (relative to Lyα) prior to the flare, and much greater than standard strengths following the flare.

In the third scenario the clouds prior to the flare have approximately standard conditions: $C \approx 0.1$, $P \approx P_{\rm std}$, $\Xi \approx \Xi_{\rm std}$, illuminated by the double power-law spectrum. Following the flare the cloud parameters would be unchanged, but the illuminating spectrum would have changed to something like the 80 eV bump spectrum discussed in the previous section. This scenario requires a change in only the extrinsic cloud properties. It has the virtue that it does not imply cloud conditions which differ greatly from the standard ones either prior to or following the flare. In particular, large covering fractions are not required; an EUV–dominated spectrum such as the 80 eV bump produces He II λ4686 at much greater efficiency than

does a double power-law spectrum. The UV resonance lines are predicted to vary in a manner similar to scenario (2): approximately standard strengths prior to the flare and large increases following the flare. Further impetus for the consideration of scenarios in which the ionizing spectrum is EUV–dominated is provided by the detection of an excess of flux in the low energy detector on the *EXOSAT* satellite (Branduardi 1986).

VI. ORIGINS OF VARIABILITY: LINE WIDTHS

The fact that the line profiles following the flare are broader than those prior to the flare complicates the discussion of the relative merits of the scenarios for line variability. This fact implies that there are two populations of clouds, and the population from which the nonlinear lines originate has a greater velocity dispersion than does the linear cloud population. In what follows we will refer to the clouds whose line fluxes vary nonlinearly as "high-velocity" clouds, and those whose line fluxes vary linearly as "low-velocity" clouds. Since cloud velocity dispersion is likely to be related to the external forces acting on the clouds it is likely that the two types of clouds are in spatially separate regions from each other, and that their differing variability behavior is due to differences in cloud parameters. If the cloud distribution is assumed to be spherically symmetric then it is clear that any change in the shape or strength of the ionizing spectrum, i.e., the extrinsic cloud properties, will eventually be felt by clouds at all velocities. Therefore, differences in the line spectra radiated by high- and low-velocity clouds must be due to one of three things: (*a*) light travel time effects; (*b*) geometric effects (departures from spherical symmetry); or (*c*) changes in the intrinsic cloud properties (i.e., pressure, covering fraction, column density, or distance from the continuum source) of one population of clouds relative to the other. One of the first two effects must be operating if the He II λ4686/Hβ increase was due to changes in the extrinsic cloud properties [i.e., scenarios (1) or (3) of the previous section]; if light travel time and geometric effects are not important, then a change in the intrinsic cloud properties (i.e., scenarios 1 or 2 of the previous section) must be the origin of the line variability in NGC 5548.

Examples of geometrical effects which could expose differing populations of clouds to different ionizing spectra include shielding by a thick accretion disk (Fabian *et al.* 1986) and limb-darkening of the radiation from a thin accretion disk (Netzer 1987). If the low-velocity clouds are at a much greater distance from the continuum source than are the high-velocity clouds, then the differing light travel times could lead to variability in the high-velocity clouds as an EUV–dominated flare reaches them. In the latter case subsequent observations should reveal that the low-velocity lines achieve the same ratios as the high-velocity lines after the flare has had time to propagate to sufficiently large distances, i.e., after ~ 1 month.

VII. SUMMARY AND CONCLUSIONS

The scenarios which could explain the line variability observed by Peterson and Ferland (1986) from NGC 5548 are as follows. (1) A large increase (more than a factor of 10, say) in cloud ionization parameter in clouds where Ξ is initially very low. This requires either a large change in cloud pressure or position or a change in the ionizing flux (but not the spectral shape). (2) An increase in the cloud covering fraction, to $C \approx 1$, of clouds with low column density, $N \approx 10^{22}$ cm^{-2}. This is the scenario favored by Peterson and Ferland. It is also able to account for the differing spectra radiated by high- and low-velocity clouds without invoking geometrical obscuration or light-travel-time effects. (3) An EUV flare incident on clouds with standard ionization parameter, pressure, column density, and covering fraction.

In the absence of observational data at both wavelengths and times adjacent to those presented by Peterson and Ferland (1986) it is impossible to argue the merits of the various explanations for the NGC 5548 variability. It is tempting to favor scenarios which do not require large departures from standard broad-line cloud parameters and which do not require changes in the intrinsic properties of clouds. The EUV flare scenario fares best according to these criteria. However, detection of simultaneous EUV or soft X-ray flaring is necessary in order to confirm this hypothesis.

We thank Gail Reichert for several stimulating discussions, and Gary Ferland and Brad Peterson for careful reading and constructive criticisms of the manuscript. One of us (M. E.) would like to thank the National Research Council for the award of a senior fellowship and the National Science Foundation for support under grant number AST-8304895.

REFERENCES

Alloin, D., Boisson, C., and Pelat, D. 1987, *Astr. Ap. Letters*, submitted.
Barr, P., Willis, A. J., and Wilson, R. 1983, *M.N.R.A.S.*, **203**, 201.
Branduardi, G. 1986, in *The Physics of Accretion onto Compact Objects*, ed. K. O. Mason (Berlin: Springer-Verlag), p. 407.
Davidson, K., and Netzer, H. 1979, *Rev. Mod. Phys.*, **51**, 715.
Elitzur, M., and Ferland, G. J. 1986, *Ap. J.*, **305**, 35.
Fabian, A. C., Guilbert, P. W., Arnaud, K. A., Shafer, R. A., Tennant, A. F., and Ward, M. J. 1986, *M.N.R.A.S.*, **218**, 457.
Ferland, G., and Shields, G. 1985, in *Astrophysics of Active Galactic Nuclei and Quasi-Stellar Objects*, ed. J. Miller (San Francisco: University Science Books), p. 157.
Krolik, J. H. 1987, in *Proc. Taos Workshop on Multiwavelength Astrophysics*, ed. F. A. Cordova (New York: American Physical Society).
Krolik, J., and Kallman, T. R. 1988, *Ap. J.*, **324**, 717.
Krolik, J. H., McKee, C. F., and Tarter, C. B. 1981, *Ap. J.*, **249**, 422.
Kwan, J. 1984, *Ap. J.*, **283**, 70.
Kwan, J., and Krolik, J. 1982, *Ap. J.*, **250**, 478.
Mushotzky, R., and Ferland, G. J. 1984, *Ap. J.*, **278**, 558.
Netzer, H. 1985, *Ap. J.*, **289**, 451.
———. 1987, *M.N.R.A.S.*, **225**, 55.
Peterson, B. M., and Ferland, G. J. 1986, *Nature*, **324**, 345.
Reichert, G., Mushotzky, R. F., Petre, R., and Holt, S. S. 1985, *Ap. J.*, **296**, 69.
Ulrich, M. H., and Boisson, C. 1983, *Ap. J.*, **267**, 515.

M. ELITZUR: Department of Physics and Astronomy, University of Kentucky, Lexington, KY 40506

T. R. KALLMAN: Code 665, NASA/Goddard Space Flight Center, Greenbelt, MD 20771